

Entanglement witnesses in the XY -chain: Thermal equilibrium and post-quench non-equilibrium states

Ferenc Iglói^{1,2,*} and Géza Tóth^{3,4,5,6,1,†}

¹*Wigner Research Centre for Physics, Institute for Solid State Physics and Optics, H-1525 Budapest, P.O. Box 49, Hungary*

²*Institute of Theoretical Physics, Szeged University, H-6720 Szeged, Hungary*

³*Department of Theoretical Physics, University of the Basque Country UPV/EHU, P.O. Box 644, E-48080 Bilbao, Spain*

⁴*EHU Quantum Center, University of the Basque Country UPV/EHU,*

Barrio Sarriena s/n, 48940 Leioa, Biscay, Spain

⁵*Donostia International Physics Center (DIPC), P.O. Box 1072, E-20080 San Sebastián, Spain*

⁶*IKERBASQUE, Basque Foundation for Science, E-48013 Bilbao, Spain*

(Dated: July 12, 2022)

Entanglement witnesses for the XY -chain are calculated, either using upper bounds of the energy of separable states or through the calculation of bipartite entanglement negativity. We obtain temperature bound for the system in thermal equilibrium and determine entangled post-quench states after a sudden quench, when the parameters of the Hamiltonian are changed rapidly. We study how these bounds are influenced by a quantum phase-transition or a disorder line in the ground state. Very strong finite-size corrections are observed in the ordered phase due to the presence of a quasi-degenerate excitation.

I. INTRODUCTION

Entanglement lies at the heart of quantum mechanics and also plays an important role in quantum information theory (QIT) [1–3]. For pure states it is equivalent to correlations, while for mixed states the two notions differ. A quantum state is entangled, if its density matrix can be written as a mixture of product states. Based on this definition, several sufficient conditions have been developed. In special cases, e.g. for 2×2 (two-qubit) and 2×3 bipartite systems [4, 5] and for multi-mode Gaussian states [6] even necessary and sufficient conditions are known.

However, in an experimental situation usually only limited information about the quantum state is available. This is true even for theoretical calculations for very large systems. Only those approaches for entanglement detection can be applied which require the measurement of a few observables. One of such approaches is using entanglement witnesses. They are observables which have a positive expectation value for all separable states. Thus a negative expectation value signals the presence of entanglement. The theory of entanglement witnesses has recently been rapidly developing [7–9]. It has been shown how to generate entanglement witnesses that detect states close to a given one, even if it is mixed or a bound entangled state [10]. It is also known how to optimize a witness operator in order to detect the most entangled states [9].

Apart from determining optimal entanglement witnesses, it is also important to find witnesses that are easy to measure in an experiment or possible to evaluate in a theoretical calculation. From both point of

views, witnesses based on spin chain Hamiltonians attracted considerable attention [11–18]. There have been already calculations for infinite chains [11, 17, 18]. It has been showed that the optimal witness for the thermal state of the chain is not necessarily the Hamiltonian [17]. Beside entanglement in general, witnesses based on energy can be used to detect multiparticle entanglement [13, 14]. Note that even a direct relation between entanglement measures and the energy of the thermal state has been observed in isotropic Heisenberg chains [19].

The energy based witnesses have been used in various physical systems such as nanotubular systems [20], in molecular nanomagnets [21], in heterometallic wheels [22], and also for theoretical calculations in theoretical spin models [23–25].

In this paper, we extend the approach to the XY model. Since the model is exactly solvable, we can make calculations for large systems. Then, we test the entanglement witness in mixed states based on the following idea. We place the system in the ground state of a given XY Hamiltonian. Then, considering a quench, we change the parameters of the Hamiltonian [26–30]. Since the state is not an eigenstate of the new Hamiltonian, dynamics start. In the infinite time limit, the system approaches a stationary state, which is some mixture of the states appearing during the dynamics. If the Hamiltonian is non-integrable, the system is expected to be thermalised and the stationary state is described by a Gibbs ensemble with an effective temperature [31–41], see however [42–45]. For integrable systems, such as the XY chain, the stationary state is assumed to be described by a so called Generalised Gibbs Ensemble (GGE) [46–53], for which different effective temperatures are assigned to each conserved quantities. This type of description has been exactly calculated for the quantum Ising chain [54], and a similar formalism is conjectured for the XY chain [55].

Here we show for the XY model that the post-quench

* igloi.ferenc@wigner.hu

† toth@alumni.nd.edu; <http://www.gtoth.eu>

state can be still handled efficiently for large systems and the expectation value of the witness operator mentioned above can also be computed. We analyze, in which cases the mixed state is detected by the witness and by the entanglement criterion based on the positivity of the partial transpose (PPT) [4, 5]. We find that the witness, even if needs few measurements, is almost as efficient as the PPT criterion.

Our paper is organized as follows. In Sec. II, we introduce the XY model, present its free-fermion representation, calculate thermal averages and present its conjectured GGE after a global quench. The entanglement witnesses are described in Sec. III. In Sec. IV, the temperature bounds are calculated both by the energy- and the entanglement negativity-methods and also finite-size corrections are studied. In Sec. V, the bounds for post-quench states are calculated. We close our paper with a discussion and conclusions in Secs. VI and VII, respectively and calculation of the thermal average of the energy in finite periodic chains is presented in the Appendix.

II. MODEL AND METHODS

In this section, we describe the model, present the XY spin-chain Hamiltonian and show how to calculate important quantities for it in free-fermion representation, including averages for finite temperature. Finally, we discuss how to handle non-equilibrium stationary states after a quench.

A. The XY-chain

The XY chain is defined by the Hamiltonian

$$\mathcal{H} = - \sum_l \left[\frac{1+\gamma}{2} \sigma_l^x \sigma_{l+1}^x + \frac{1-\gamma}{2} \sigma_l^y \sigma_{l+1}^y \right] - h \sum_l \sigma_l^z \quad (1)$$

in terms of the Pauli spin operators $\sigma_l^{x,y,z}$ at site $l = 1, \dots, L-1$. Generally, we consider large finite chains of length L with periodic boundary conditions. The parameters $0 \leq \gamma \leq 1$ and $h \geq 0$ denote the strength of the anisotropy and the transverse field, respectively. The special case $\gamma = 1$ represents the transverse Ising model, and for $h = 0, \gamma = 0$ the Hamiltonian reduces to the XX chain (see the equilibrium phase diagram in Fig. 1).

B. Free-fermion representation

Using standard techniques [56, 57], the Hamiltonian in Eq. (1) is expressed in terms of fermion creation and annihilation operators η_p^\dagger and η_p as

$$\mathcal{H} = \sum_p \varepsilon(p) \left(\eta_p^\dagger \eta_p - \frac{1}{2} \right), \quad (2)$$

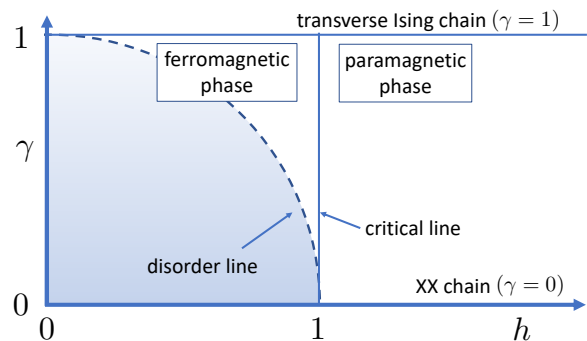


FIG. 1. Phase diagram of the XY chain. In the oscillatory region, $h^2 + \gamma^2 < 1$, denoted by the shaded (blue) part the bipartite entanglement negativity eigenvalues satisfy: $\mu_{\min}^{(1)} < \mu_{\min}^{(2)}$. Outside this region the bipartite entanglement witness can be expressed through nearest neighbour correlations, see in Eq. (34).

where the sum runs over L quasi-momenta, which are equidistant in $[-\pi, \pi]$ for periodic boundary conditions and almost equidistant in $[0, \pi]$ for free boundary conditions and finite L , but again equidistant in the limit $L \rightarrow \infty$. The energy of the modes is given by [26, 27, 55]

$$\varepsilon(p) = 2\sqrt{\gamma^2 \sin^2 p + (h - \cos p)^2} \quad (3)$$

and the Bogoliubov angle Θ_p diagonalizing the Hamiltonian is given by $\tan \Theta_p = -\gamma \sin p / (h - \cos p)$.

The energy of the ground state is given as

$$E_0 = - \sum_p \frac{\varepsilon(p)}{2}. \quad (4)$$

1. Disorder line $h_d^2 + \gamma^2 = 1$

The system has special behavior at the disorder line $h_d^2 + \gamma^2 = 1$. Here the energy of modes has the simple form

$$\varepsilon(p) = 2(1 - h_d \cos p), \quad h_d^2 + \gamma^2 = 1, \quad (5)$$

and the ground-state energy density in the thermodynamic limit is given by:

$$\frac{E_0}{L} = -\frac{1}{\pi} \int_0^\pi (1 - h_d \cos p) dp = -1, \quad h_d^2 + \gamma^2 = 1. \quad (6)$$

Below the disorder line, $h^2 + \gamma^2 < 1$, the long-range correlation functions have an oscillatory behavior, whereas at the disorder line these are constant.

C. Averages at finite temperature

Here the results are given in the thermodynamic limit, $L \rightarrow \infty$. Calculations of the energy for finite periodic chains are presented in the Appendix.

1. Energy

At finite temperature, $T > 0$, the partition function is expressed as:

$$Z = 2^L \prod_p \cosh \left(\frac{\varepsilon(p)}{2T} \right), \quad (7)$$

and the average value of the energy is given by:

$$\langle \mathcal{H} \rangle_T = - \sum_p t(p, T) \frac{\varepsilon(p)}{2}, \quad (8)$$

with

$$t(p, T) = \tanh \left(\frac{\varepsilon(p)}{2T} \right). \quad (9)$$

in units $k_B = 1$.

2. Correlation functions

The correlation functions of the XY-model are calculated in [26, 27] and the nearest neighbour correlations can be expressed as

$$\begin{aligned} \langle \sigma_i^x \sigma_{i+1}^x \rangle_T &= g_c - g_s, \\ \langle \sigma_i^y \sigma_{i+1}^y \rangle_T &= g_c + g_s, \\ \langle \sigma_i^z \sigma_{i+1}^z \rangle_T &= g_0^2 - g_c^2 + g_s^2 \end{aligned} \quad (10)$$

through

$$\begin{aligned} g_c &= \frac{1}{L} \sum_p \cos p (\cos p - h) t(p, T) \varepsilon^{-1}(p), \\ g_s &= -\gamma \frac{1}{L} \sum_p \sin^2 p t(p, T) \varepsilon^{-1}(p), \\ g_0 &= \frac{1}{L} \sum_p (h - \cos p) t(p, T) \varepsilon^{-1}(p). \end{aligned} \quad (11)$$

We stress once more that these relations are valid in the thermodynamic limit, $L \rightarrow \infty$. One can easily check, that:

$$-\frac{1+\gamma}{2} \langle \sigma_i^x \sigma_{i+1}^x \rangle_T - \frac{1-\gamma}{2} \langle \sigma_i^y \sigma_{i+1}^y \rangle_T - h \langle \sigma_i^z \rangle_T = \frac{1}{L} \langle H \rangle_T \quad (12)$$

with $\langle \sigma_i^z \rangle_T = g_0$, as it should be.

D. Non-equilibrium stationary states after a quench

We consider global quenches (at zero temperature), which suddenly change the parameters of the Hamiltonian from γ_0, h_0 for $t < 0$ to γ, h for $t > 0$. For $t < 0$ the system is assumed to be in equilibrium, i.e. in the

ground state of the Hamiltonian \mathcal{H} with parameters γ_0 and h_0 , which is denoted by $|\Phi_0\rangle$. After the quench, for $t > 0$, the state evolves coherently according to the new Hamiltonian as

$$|\Phi_0(t)\rangle = \exp(-i\mathcal{H}t) |\Phi_0\rangle. \quad (13)$$

Correspondingly the time evolution of an operator in the Heisenberg picture is

$$\sigma_l(t) = \exp(i\mathcal{H}t) \sigma_l \exp(-i\mathcal{H}t). \quad (14)$$

The energy of the system after the quench is given by:

$$\langle \Phi_0 | \mathcal{H} | \Phi_0 \rangle = \sum_p \varepsilon(p) \left(\langle \Phi_0 | \eta_p^\dagger \eta_p | \Phi_0 \rangle - \frac{1}{2} \right), \quad (15)$$

where $f_p = \langle \Phi_0 | \eta_p^\dagger \eta_p | \Phi_0 \rangle$ is the occupation probability of mode p in the initial state $|\Phi_0\rangle$. For the XY model it is expressed through the difference $\Delta_p = \Theta_p^0 - \Theta_p$ of the Bogoliubov angles as $f_p = \frac{1}{2} (1 - \cos \Delta_p)$ with

$$\cos \Delta_p = \frac{(\cos p - h_0)(\cos p - h) + \gamma \gamma_0 \sin^2 p}{\varepsilon(p) \varepsilon_0(p)}, \quad (16)$$

where the index 0 refers to quantities before the quench [55].

After large enough time and in the thermodynamic limit the system is expected to reach a stationary state, in which - due to conserved symmetries - averages of correlations are described by a generalised Gibbs ensemble (GGE)[46–53]. In this case to each fermionic mode an effective temperature, $T_{\text{eff}}(p)$ is attributed through the relation [55]:

$$\tanh \left(\frac{\varepsilon(p)}{2T_{\text{eff}}(p)} \right) = |2f_p - 1| = |\cos \Delta_p|. \quad (17)$$

This follows by comparing the relations in Eqs.(8),(9) and (15). In this way the nearest neighbour correlations in the stationary state can be obtained as in section II C, just changing the factor in Eq. (9) as

$$t(p, T) \rightarrow |\cos \Delta_p|. \quad (18)$$

This relation applies also for the correlation functions in Eqs.(10,11).

III. ENTANGLEMENT WITNESSES

Generally an operator \mathcal{W} is called an entanglement witness, if its expectation value, $\langle \mathcal{W} \rangle$ satisfies the following requirements [58, 59]: (i) $\langle \mathcal{W} \rangle \geq 0$ for all separable states, (ii) $\langle \mathcal{W} \rangle < 0$ for some entangled state. Here we present the energy based witness [11] and the bipartite entanglement negativity witness [17] what we will use to analyse the entanglement properties of the XY-chain.

A. Energy witness

In this section, we review the idea of detecting entanglement with energy measurement [11].

First we calculate the minimum of $\langle \mathcal{H} \rangle$ for separable states, which are considered in the product form:

$$|\Psi\rangle = |\psi\rangle_1 \otimes |\psi\rangle_2 \otimes \cdots \otimes |\psi\rangle_L, \quad (19)$$

with

$$|\psi\rangle_k = \cos \phi e^{i\theta_\uparrow} |\uparrow\rangle_k + \sin \phi e^{i\theta_\downarrow} |\downarrow\rangle_k. \quad (20)$$

The energy per site of this state is given by:

$$\frac{1}{L} \langle \Psi | \mathcal{H} | \Psi \rangle = -\frac{1}{2} \sin^2 2\phi [1 + \gamma \cos 2(\theta_\uparrow - \theta_\downarrow)] - h \cos 2\phi. \quad (21)$$

having the minimum at $\theta_\uparrow = \theta_\downarrow$ and for

$$\begin{aligned} \cos 2\phi &= \frac{h}{1+\gamma}, & \text{for } h &\leq 1+\gamma, \\ \phi &= 0, & \text{for } h &> 1+\gamma. \end{aligned} \quad (22)$$

Thus the minimum energy per site for product states is given by:

$$\frac{1}{L} E_{\text{sep}} = \begin{cases} -\frac{(1+\gamma)^2 + h^2}{2(1+\gamma)}, & \text{for } h \leq 1+\gamma, \\ -h, & \text{for } h > 1+\gamma. \end{cases} \quad (23)$$

This expression is also the bound for separable quantum mixed states, for which the density matrix is written as

$$\rho_{\text{sep}} = \sum_m p_m \rho_m^{(1)} \otimes \rho_m^{(2)} \otimes \cdots \otimes \rho_m^{(L)}, \quad (24)$$

where $\rho_m^{(k)}$ are single particle pure states. This follows from the fact that the expectation value $\langle \mathcal{H} \rangle = \text{Tr}(\rho H)$ is linear in ρ . Then we can simply write

$$\langle \mathcal{W}_E \rangle = \langle \mathcal{H} \rangle - E_{\text{sep}} \quad (25)$$

where the averages can be either for thermal states (see in Eq. (8)) or for post-quench states [see in Eq. (15)].

Along the disorder line, $h^2 + \gamma^2 = 1$ we have for the bound: $E_{\text{sep}} = E_0 = -L$, thus the state is separable at this line.

B. Bipartite entanglement negativity witness

In this section, we summarize the method presented in Ref. [17]. It suggests to use not the Hamiltonian but another operator as an entanglement witness for spin chains in thermal equilibrium, which is shown to be connected to the partial transpose of the density matrix [4, 5].

Let us consider the nearest neighbour reduced density matrix, ρ , which will be defined in the σ^z basis: $|\alpha\rangle = |\uparrow\rangle$ or $|\alpha\rangle = |\downarrow\rangle$ and using the convention $|\uparrow\uparrow\rangle = |1\rangle$,

$|\uparrow\downarrow\rangle = |2\rangle$, $|\downarrow\uparrow\rangle = |3\rangle$ and $|\downarrow\downarrow\rangle = |4\rangle$. Due to symmetry \mathcal{H} , as well as ρ has two orthogonal subspaces, which are spanned by the states: $|1\rangle, |4\rangle$ and $|2\rangle, |3\rangle$, respectively. Consequently in terms of non-zero elements it is represented as

$$\rho = \begin{bmatrix} \rho_{11} & 0 & 0 & \rho_{14} \\ 0 & \rho_{22} & \rho_{23} & 0 \\ 0 & \rho_{32} & \rho_{33} & 0 \\ \rho_{41} & 0 & 0 & \rho_{44} \end{bmatrix}. \quad (26)$$

The matrix is real and symmetric, $\rho_{14} = \rho_{41}$ and $\rho_{23} = \rho_{32}$, furthermore $\rho_{11} + \rho_{22} + \rho_{33} + \rho_{44} = 1$.

A bipartite entanglement measure is the negativity:

$$\mathcal{N}(\rho) = 2 \max(0, -\min(\mu_\nu)), \quad (27)$$

where μ_ν are the eigenvalues of the partial transpose ρ^{TA} of ρ , defined by the matrix-elements $\rho_{\alpha\beta, \gamma\delta}^{TA} = \rho_{\gamma\beta, \alpha\delta}$. By indicating the zero elements explicitly, we obtain

$$\rho^{TA} = \begin{bmatrix} \rho_{11} & 0 & 0 & \rho_{23} \\ 0 & \rho_{22} & \rho_{14} & 0 \\ 0 & \rho_{41} & \rho_{33} & 0 \\ \rho_{32} & 0 & 0 & \rho_{44} \end{bmatrix}. \quad (28)$$

The lowest eigenvalue of ρ^{TA} , denoted by μ_{\min} is non-negative if and only if the state is separable. According to Eq. (28) μ_{\min} can be in one of two orthogonal sectors:

$$\begin{aligned} \mu_{\min}^{(1)} &= \frac{1}{2} \left[\rho_{11} + \rho_{44} - \sqrt{(\rho_{11} - \rho_{44})^2 + 4\rho_{23}\rho_{32}} \right], \\ \mu_{\min}^{(2)} &= \frac{1}{2} \left[\rho_{22} + \rho_{33} - \sqrt{(\rho_{22} - \rho_{33})^2 + 4\rho_{14}\rho_{41}} \right]. \end{aligned} \quad (29)$$

We have checked numerically in finite systems, that in the oscillatory region, $h^2 + \gamma^2 < 1$, $\mu_{\min}^{(1)} < \mu_{\min}^{(2)}$, while for $h^2 + \gamma^2 > 1$ it is the opposite: $\mu_{\min}^{(2)} < \mu_{\min}^{(1)}$. At the disordered line, $h^2 + \gamma^2 = 1$ we have $\mu_{\min}^{(1)} = \mu_{\min}^{(2)}$ and here the state is separable even at $T = 0$.

Regarding $\mu_{\min}^{(2)}$ here $\rho_{22} = \rho_{33}$, consequently

$$\mu_{\min}^{(2)} = \rho_{22} - \rho_{14}. \quad (30)$$

These matrix elements of ρ can be expressed through nearest neighbour correlations:

$$\begin{aligned} \langle \sigma_i^z \sigma_{i+1}^z \rangle - 1 &= \rho_{11} - \rho_{22} - \rho_{33} + \rho_{44} \\ -(\rho_{11} + \rho_{22} + \rho_{33} + \rho_{44}) &= -2(\rho_{22} + \rho_{33}) = -4\rho_{22} \end{aligned} \quad (31)$$

and

$$\begin{aligned} \langle \sigma_i^x \sigma_{i+1}^x \rangle - \langle \sigma_i^y \sigma_{i+1}^y \rangle &= 2(\langle \sigma_i^+ \sigma_{i+1}^+ \rangle + \langle \sigma_i^- \sigma_{i+1}^- \rangle) \\ &= 2(\rho_{14} + \rho_{41}) = 4\rho_{14}, \end{aligned} \quad (32)$$

thus

$$\mu_{\min}^{(2)} = -\frac{1}{4} (\langle \sigma_i^x \sigma_{i+1}^x \rangle - \langle \sigma_i^y \sigma_{i+1}^y \rangle + \langle \sigma_i^z \sigma_{i+1}^z \rangle - 1). \quad (33)$$

Consequently in the regime, where $\mu_{\min}^{(2)} < \mu_{\min}^{(1)}$ the expectation value of the operator

$$\mathcal{W}_N = -\frac{1}{4}(\sigma_i^x \sigma_{i+1}^x - \sigma_i^y \sigma_{i+1}^y + \sigma_i^z \sigma_{i+1}^z - 1) \quad (34)$$

gives the lowest eigenvalue of the partial transpose for the XY-chain. Evidently, \mathcal{W}_N is an entanglement witness, since it is non-negative on product states and $\mathcal{W}_N = -1/2$ for the maximally entangled state

$$\frac{1}{\sqrt{2}}(|\uparrow\uparrow\rangle + |\downarrow\downarrow\rangle). \quad (35)$$

Here we note that the partial transposition of a two-qubit state has at most one negative eigenvalue and all the eigenvalues lie in $[-1/2, 1]$ [61, 62].

IV. TEMPERATURE BOUNDS FOR EQUILIBRIUM THERMAL STATES

In this section we consider thermal states, which are generally entangled at low temperature, but at sufficiently high temperature these are separable. Using different type of entanglement witnesses we calculate temperature bounds, say T_E [for energy based witness Eq. (33)] and T_N [for entanglement negativity witness Eq. (34)], below which bounds the state is detected entangled. We note that at specific points there have been calculations for infinite chains [11, 17, 18]. Here we consider several parts of the phase diagram and also study the finite size corrections that turn out to be very important in the ordered phase.

A. Energy bound

1. Thermodynamic limit

According to the energy bound thermal states are detected entangled, if $\mathcal{W}_E < 0$, thus $\langle H \rangle_T < E_{\text{sep}}$, which is valid for $T < T_E$. In Fig. 2 we show T_E as a function of h , for different values of the anisotropy, which is calculated in the thermodynamic limit. Starting in the paramagnetic phase, $h > 1$, here T_E monotonously decreases with γ , and it is $T_E \rightarrow 0$ as $\gamma \rightarrow 0$. At a fixed $1 \geq \gamma > 0$, T_E also decreases with decreasing h and passing through the critical point in the ordered phase approaches zero at the disorder point

$$h_d = \sqrt{1 - \gamma^2}. \quad (36)$$

Decreasing h further at the other side of the disorder point the temperature bound start to increase monotonously. With $h = 0$, the order of the $T_E(\gamma)$ values is the opposite of that with $h > 1$. At the disorder point there is a singularity

$$T_E \sim \ln^{-1} |h - h_d|. \quad (37)$$

Regarding the quantum critical point, $h = 1$, close to it there is an inflection point of the $T_E(h)$ curve, the position of which approaches $h = 1$ as $\gamma \rightarrow 0$.

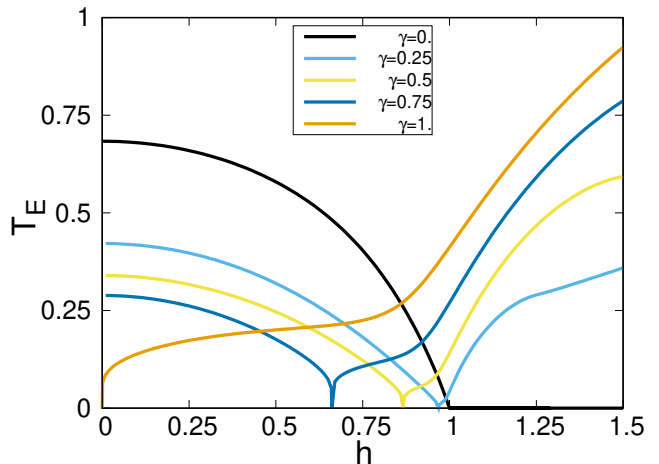


FIG. 2. Temperature bound of entangled equilibrium thermal states in the thermodynamic limit calculated through the energy bound. At the disorder point, $h_d = \sqrt{1 - \gamma^2}$ the state is separable and $T_E = 0$.

2. Finite-size corrections

We have repeated the calculation of the temperature bound on finite transverse Ising chains working in the Ising spin basis, in this way we went up to $L = 12$. Results are shown in the main panel of Fig. 3. The corrections are relatively small in the paramagnetic phase, but in the ordered phase these are quite strong. To see more precisely the finite-size dependence of the correction term we repeated the calculation in the free-fermion basis as described in Sec..

We have studied the finite-size dependence of the correction term, $\Delta T_E(L) = T_E(L) - T_E$, at different points of the phase diagram. For points in the ordered phase ($h = 0.25, 0.5$ and 0.75) these are shown in the upper inset of Fig. 3, while at the critical point ($h = 1.0$) and in the paramagnetic phase ($h = 1.25$) these are in the lower inset. Using lin-log scale in the figures the curves are asymptotically linear, thus the size-dependence is well described by the form:

$$\Delta T_E(L) \simeq AL^{-a} \exp(-L/L_0), \quad (38)$$

where the power-law correction term is relevant for short chains, $L < L_0$. In the paramagnetic phase and at the critical point L_0 is just a few lattice spacing, while in the ferromagnetic phase it is much longer and tends to infinity at $h \rightarrow 0$. The slow finite-size convergence of the results is due to the presence of an exponentially small gap in the ordered phase, which has a large correction.

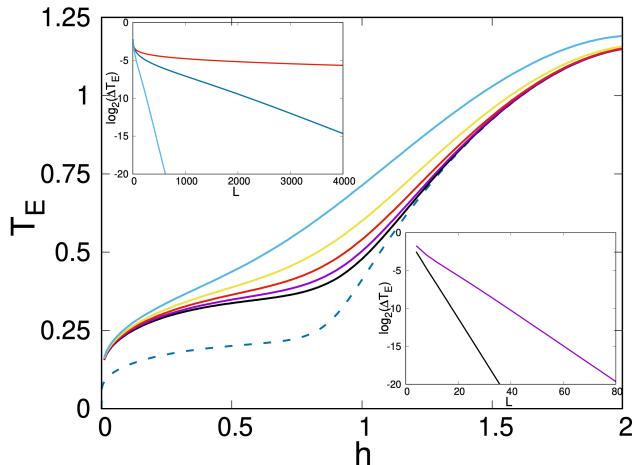


FIG. 3. Main panel: temperature bound of entangled equilibrium thermal states in finite transverse Ising chains calculated through the energy bound, with $L = 4, 6, 8, 10, 12$ up to down and $L \rightarrow \infty$ indicated by the dashed line. Inset: finite-size corrections in a lin-log scale at different values of h . Upper inset: corrections in the ordered phase with $h = 0.25, 0.5$ and 0.75 , up to down. Lower inset: at the critical point $h = 1.0$ (up) and in the paramagnetic phase $h = 1.25$ (down). (Note the different scales in the x -axis.)

B. Entanglement negativity bound

We have calculated the temperature bound, T_N , using the entanglement negativity criterion in Eq. (27). Results for the transverse Ising chain are in the main panel of Fig. 4 both for finite chains (calculated in the Ising spin bases) and in the thermodynamic limit using nearest neighbour correlations in Eq. (33). Comparing the results with those obtained with the energy bound a higher limiting temperature is obtained by the entanglement negativity criterion; the difference is around a factor of two. With regard to the finite-size corrections, these appear almost negligible in the paramagnetic phase, but are considerably strong in the ferromagnetic phase. The origin of the strong corrections is due to the quasi-degenerate ground state, as discussed in the previous paragraph.

We have repeated the calculation for different values of $0 < \gamma < 1$, the results for $\gamma = 0.8$ are shown in the upper inset of Fig. 4 and for $\gamma = 0.6$ in the lower inset. Here the calculation of the infinite chain limit through the nearest neighbour correlations in Eq. (33) is feasible for

$$h > h_d = \sqrt{1 - \gamma^2}. \quad (39)$$

In these cases too, the convergence to the thermodynamic limit is very fast in the paramagnetic phase, while in the ferromagnetic phase the convergence is much slower. Comparing the results with those obtained from the energy bound the entanglement negativity bounds are considerably higher.

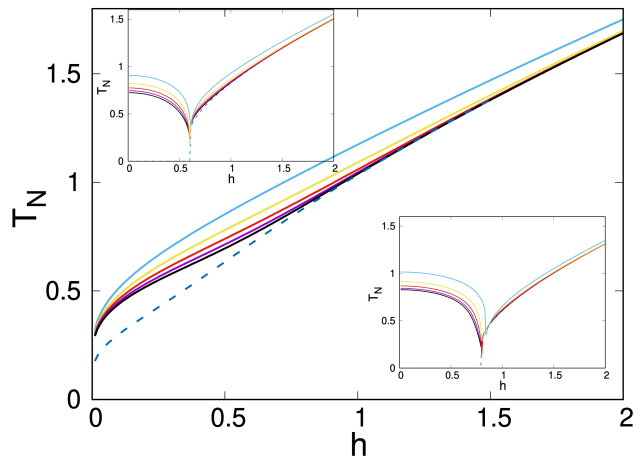


FIG. 4. Temperature bound of entangled equilibrium thermal states in finite XY chains calculated through the entanglement bound, with $L = 4, 6, 8, 10, 12$ up to down and $L \rightarrow \infty$ indicated by the dashed line. Main panel: $\gamma = 1$, quantum Ising chain; upper inset: $\gamma = 0.8$; lower inset: $\gamma = 0.6$. In the thermodynamical limit the results are valid for $h > h_d = \sqrt{1 - \gamma^2}$.

V. ENTANGLEMENT IN NON-EQUILIBRIUM POST-QUENCH STATES

In this section we consider global quenches in the system, as described in Section IID and study the entanglement properties of non-equilibrium stationary states, which are obtained in the large time limit after the quench. To calculate averages we use the GGE protocol and assign different effective temperatures to each fermionic modes, as described in Eqs.(17,18). First we apply the energy based witness in Eq. (33) and then the entanglement negativity witness in Eq. (34).

A. Energy bound

The energy based witness detects the post-quench state entangled provided: $\langle \Phi_0 | \mathcal{H} | \Phi_0 \rangle < E_{\text{sep}}$. This defines bounds which are expressed with the parameters of the Hamiltonian before and after the quench. In the following, for simplicity we consider fixed values of $\gamma_0 = \gamma$ and study the area of detected entanglement in the (h_0, h) plane. To calculate the boundary of this area one should analyse separately to two equations in Eq. (23).

(i) If $h \leq 1 + \gamma$ then

$$-hI_1(h_0, \gamma) - I_2(h_0, \gamma) = -\frac{(1 + \gamma)^2 + h^2}{4(1 + \gamma)}, \quad (40)$$

with

$$\begin{aligned}
I_1(h_0, \gamma) &= \frac{1}{2\pi} \int_0^\pi \frac{h_0 - \cos p}{\sqrt{\gamma^2 \sin^2 p + (h_0 - \cos p)^2}} dp, \\
I_2(h_0, \gamma) &= \frac{1}{2\pi} \int_0^\pi \frac{-h_0 \cos p + \cos^2 p + \gamma^2 \sin^2 p}{\sqrt{\gamma^2 \sin^2 p + (h_0 - \cos p)^2}} dp.
\end{aligned} \tag{41}$$

The solution of Eq. (40) defines the boundaries

$$h_\pm = \left(I_1 \pm \sqrt{I_1^2 + I_2/(1+\gamma) - 1/4} \right) 2(1+\gamma). \tag{42}$$

(ii) If $h > 1 + \gamma$ then we have to consider the following case. Using this equation it modifies only the upper boundary in Eq.(42) (since $h_- < 1 + \gamma$), which is given now

$$h_+ = \frac{I_2}{1 - 2I_1}. \tag{43}$$

The region in which the post-quench states are detected entangled are presented in Fig. 5 with a yellow filled area. This consists of two connected parts, which touch each other at the disorder point,

$$h = h_0 = h_d = \sqrt{1 - \gamma^2}. \tag{44}$$

Note that for the quantum Ising chain with $\gamma = 1$ we have just one connected part.

If the initial state is in the ferromagnetic domain, $h_0 < 1$, the region of post-quenched states detected as entangled is rather narrow, the possible values of h are close to h_0 . Starting the quench from the paramagnetic phase, $h_0 > 1$ the the domain of post-quench states detected entangled becomes relatively wider. Starting the quench just at the critical point, $h_0 = 1$, the boundaries exhibit a singularity:

$$\frac{dh_\pm}{dh_0} \sim -(h_\pm - 1) \ln |h_0 - 1|. \tag{45}$$

B. Entanglement negativity bound

We have calculated the region of post-quenched states detected as entangled by the entanglement negativity method, which gives proper bounds in the region, where $\mu_{\min}^{(2)} < \mu_{\min}^{(1)}$. Results are shown in the panels of Fig. 5 as filled grey areas (having also the included yellow parts). For the transverse Ising chain (see in the first panel of Fig. 5) this method is applicable in the whole phase diagram. For $\gamma < 1$ the condition $\mu_{\min}^{(2)} < \mu_{\min}^{(1)}$ is valid just in a part of the phase diagram. According to the numerical results no entangled post-quenched states are detected in the region $h < h_d, h_0 < h_d$ with

$$h_d = \sqrt{1 - \gamma^2}. \tag{46}$$

Generally, the entangled region detected by the negativity witness is larger, than that detected by the energy based witness. We noticed that the border of the entangled domain is singular at the critical point of the system before the quench: $h_0 = 1$.

VI. DISCUSSION

Entanglement in mixed quantum states is a difficult problem, in particular when the degrees of freedom is large and we approach the thermodynamic limit. The possible systems of investigation are usually quantum spin systems, most often quantum spin chains. Such type of quantum spin chains could have experimental realisations or they could be manufactured artificially through ultra-cold atomic gases in an optical lattice. Recently, this latter type technique is very well developed and different intriguing questions could be studied experimentally [63–71]. One such problem is related to the quantum quench, when parameters of the Hamiltonian of the system is changed abruptly and the time-evolution of the system is governed by the new Hamiltonian. After sufficiently long time the system will approach a non-equilibrium stationary state, the properties of which are of vital importance. This post-quench state is a mixed quantum state. For general, non-integrable system it is expected a thermal state, which is described by an appropriate Gibbs ensemble. For integrable systems, for which examples are the XXZ or the XY chains, the post-quenched state is described by a so called Generalised Gibbs Ensemble.

In this paper we consider the XY chain, which is integrable through free-fermionic techniques and several exact results are available, mainly in the ground state but there are some known results even at finite temperature [26, 27]. We consider the entanglement properties of mixed states of the XY chain. To detect entanglement we use different entanglement witnesses: one, which is related to the energy bound and the other, which uses bipartite entanglement negativity. Using the former is technically simpler, but doesn't detect all kind of entanglement. In contrast the bipartite entanglement negativity detects all kind of entanglement, but it is generally more complicated to calculate and often can't explore the whole phase of parameters.

One set of mixed states are thermal ones, for which some previous calculations are available at specific points for infinite chains [11, 17, 18]. Here we performed the entanglement detection both for finite chains and in the thermodynamic limit. In the ordered phase of the system very strong finite-size corrections are detected, which are due to the presence of a quasi-degenerate first excited state, having a gap, which is exponentially small with the length of the chain.

The main novelty of the the present paper is that we considered also mixed states which are due to a quench. We observed, that the post-quenched state has an entan-

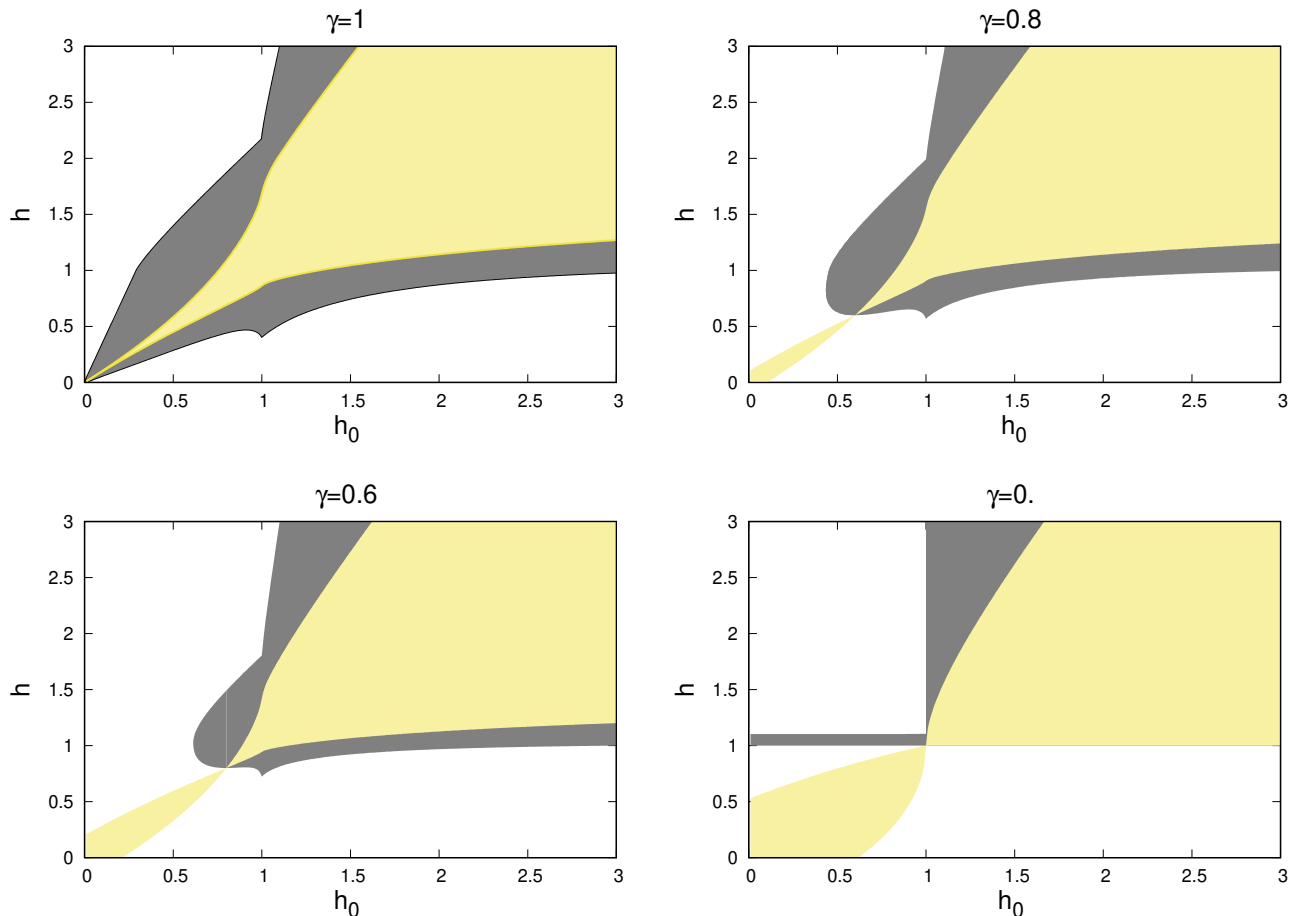


FIG. 5. Entangled post-quench states (filled area: grey - entanglement negativity bound, yellow: energy bound) after a sudden quench protocol: $(h_0, \gamma) \rightarrow (h, \gamma)$ in the XY chain. The entanglement negativity witness is not applicable in the left-down corner of the diagram: $h < h_d, h_0 < h_d$ with $h_d = \sqrt{1 - \gamma^2}$.

gled two-qubit reduced state for the nearest neighbors, if the parameters involved during the quench (in our case the transverse fields h and h_0) are sufficiently close to each others. If the parameters are changed a large extent, then the nearest neighbor two-qubit reduced state for the non-equilibrium stationary state becomes non-entangled. We expect that the latter statement is generally valid for the entanglement of non-equilibrium post-quenched states. It would be interesting to check the entanglement properties of post-quenched states of other (Bethe-Ansatz) integrable models.

VII. CONCLUSIONS

We used energy-based entanglement witnesses to detect entanglement in the thermal states of the infinite and finite XY chain, as well as in the mixed states arising after quench. We considered systems in the thermodynamic limit as well as finite systems. We compared their performance to the entanglement criterion based on the

negativity of the partial transpose. We find that they efficiently detect entanglement, while the computational effort is modest in their evaluation.

ACKNOWLEDGMENTS

We thank I. Apellaniz, I. L. Egusquiza, C. Klempt, J. Kołodyński, G. Muga, J. Siewert, Sz. Szalay, and G. Vitagliano for discussions. This work was supported by the National Research Fund under Grants No. K128989 and No. KKP-126749. We acknowledge the support of the EU (COST Action CA15220, QuantERA CEBBEC, QuantERA MENTA, QuantERA, QuSiED), the Spanish MCIU (Grant No. PCI2018-092896), the Grant PGC2018-101355-B-I00 funded by MCIN/AEI/10.13039/501100011033 and by "ERDF A way of making Europe", the Basque Government (Grant No. IT986-16). We thank the "Frontline" Research Excellence Programme of the NKFIH (Grant No. KKP133827). G. T. thanks a Bessel Research Award of

the Humboldt Foundation.

Appendix: Thermal average of the energy for finite periodic chains

For periodic chains in the fermionic representation there are two sectors, depending on the parity of the number of fermions [72, 73].

(i) For *even number of fermions*, let us denote the Hamiltonian by $\mathcal{H}^{(+)}$, the possible values of the momenta are:

$$p = \pm \frac{\pi}{L}(2m - 1), \quad m = 1, 2, \dots, L/2. \quad (\text{A.1})$$

(ii) For *odd number of fermions*, let us denote the Hamiltonian by $\mathcal{H}^{(-)}$, the possible values of the momenta are:

$$q = 0, \pi, \pm \frac{2\pi}{L}n, \quad n = 1, 2, \dots, L/2 - 1. \quad (\text{A.2})$$

In this sector the energy of the $q = 0$ mode is specific

$$\varepsilon(q = 0) = 2(h - 1). \quad (\text{A.3})$$

The partition function of the system is given as

$$Z = Z^{(+)} + Z^{(-)}, \quad (\text{A.4})$$

where $Z^{(\pm)}$ are the partition functions calculated with even and odd number of fermions, respectively.

The even partition function for $L = 2\ell$ sites is given by:

$$Z_{2\ell}^{(+)} = 2^{2\ell-1} \left[\prod_{p>0} \cosh^2 \left(\frac{\beta\varepsilon(p)}{2} \right) + \prod_{p>0} \sinh^2 \left(\frac{\beta\varepsilon(p)}{2} \right) \right], \quad (\text{A.5})$$

and the analogous odd partition function is expressed as

$$Z_{2\ell}^{(-)} = 2^{2\ell-2} \left[C^{(+)} \prod_{0<q<\pi} \cosh^2 \left(\frac{\beta\varepsilon(q)}{2} \right) + C^{(-)} \prod_{0<q<\pi} \sinh^2 \left(\frac{\beta\varepsilon(q)}{2} \right) \right], \quad (\text{A.6})$$

with the definitions

$$C^{(\pm)} = \cosh(\beta) \pm \cosh(\beta h). \quad (\text{A.7})$$

The thermal average of the energy is given by

$$\langle \mathcal{H} \rangle_T = \langle \mathcal{H}^{(+)} \rangle_T \frac{1}{1 + Z^{(-)}/Z^{(+)}} + \langle \mathcal{H}^{(-)} \rangle_T \frac{Z^{(-)}/Z^{(+)}}{1 + Z^{(-)}/Z^{(+)}} , \quad (\text{A.8})$$

with

$$\langle \mathcal{H}^{(+)} \rangle_T = \frac{\partial \ln Z^{(+)}}{\partial \beta} = \sum_{p>0} \varepsilon(p) \left[\tanh \left(\frac{\beta\varepsilon(p)}{2} \right) \frac{1}{1 + T^{(p)}} + \coth \left(\frac{\beta\varepsilon(p)}{2} \right) \frac{T^{(p)}}{1 + T^{(p)}} \right]. \quad (\text{A.9})$$

Similarly, we have

$$\langle \mathcal{H}^{(-)} \rangle_T = \frac{\partial \ln Z^{(-)}}{\partial \beta} = \frac{S^{(+)} + S^{(-)} T^{(q)}}{C^{(+)} + C^{(-)} T^{(q)}} + \sum_q \varepsilon(q) \left[\tanh \left(\frac{\beta\varepsilon(q)}{2} \right) \frac{1}{1 + T^{(q)} C^{(-)}/C^{(+)}} + \coth \left(\frac{\beta\varepsilon(q)}{2} \right) \frac{T^{(q)} C^{(-)}/C^{(+)}}{1 + T^{(q)} C^{(-)}/C^{(+)}} \right]. \quad (\text{A.10})$$

Here

$$T^{(p)} = \prod_{p>0} \tanh^2 \left(\frac{\beta\varepsilon(p)}{2} \right), \quad T^{(q)} = \prod_{0<q<\pi} \tanh^2 \left(\frac{\beta\varepsilon(q)}{2} \right), \quad (\text{A.11})$$

and

$$S^{(\pm)} = \sinh(\beta) \pm h \sinh(\beta h). \quad (\text{A.12})$$

-
- [1] R. Horodecki, P. Horodecki, M. Horodecki, and K. Horodecki, Quantum entanglement, *Rev. Mod. Phys.* **81**, 865 (2009).
 [2] O. Gühne and G. Tóth, Entanglement detection, *Phys. Rep.* **474**, 1 (2009).
 [3] N. Friis, G. Vitagliano, M. Malik, and M. Huber, Entanglement certification from theory to experiment, *Nat. Rev. Phys.* **1**, 72 (2019).
 [4] A. Peres, Separability criterion for density matrices, *Phys. Rev. Lett.* **77**, 1413 (1996).
 [5] P. Horodecki, Separability criterion and inseparable

- mixed states with positive partial transposition, *Phys. Lett. A* **232**, 333 (1997).
 [6] G. Giedke, B. Kraus, M. Lewenstein, and J. I. Cirac, Entanglement criteria for all bipartite Gaussian states, *Phys. Rev. Lett.* **87**, 167904 (2001).
 [7] M. Horodecki, P. Horodecki, and R. Horodecki, Separability of mixed states: necessary and sufficient conditions, *Phys. Lett. A* **223**, 1 (1996).
 [8] B. M. Terhal, Bell inequalities and the separability criterion, *Phys. Lett. A* **271**, 319 (2000).
 [9] M. Lewenstein, B. Kraus, J. I. Cirac, and P. Horodecki,

- Optimization of entanglement witnesses, *Phys. Rev. A* **62**, 052310 (2000).
- [10] A. Acín, D. Bruß, M. Lewenstein, and A. Sanpera, Classification of mixed three-qubit states, *Phys. Rev. Lett.* **87**, 040401 (2001).
- [11] G. Tóth, Entanglement witnesses in spin models, *Phys. Rev. A* **71**, 010301(R) (2005).
- [12] G. Tóth and O. Gühne, Detection of multipartite entanglement with two-body correlations, *Appl. Phys. B* **82**, 237 (2006).
- [13] O. Gühne and G. Tóth, Energy and multipartite entanglement in multidimensional and frustrated spin models, *Phys. Rev. A* **73**, 052319 (2006).
- [14] O. Gühne, G. Tóth, and H. J. Briegel, Multipartite entanglement in spin chains, *New J. Phys.* **7**, 229 (2005).
- [15] C. Brukner and V. Vedral, Macroscopic Thermodynamical Witnesses of Quantum Entanglement, *arXiv: quant-ph/0406040* (2004).
- [16] M. R. Dowling, A. C. Doherty, and S. D. Bartlett, Energy as an entanglement witness for quantum many-body systems, *Phys. Rev. A* **70**, 062113 (2004).
- [17] L.-A. Wu, S. Bandyopadhyay, M. S. Sarandy, and D. A. Lidar, Entanglement observables and witnesses for interacting quantum spin systems, *Phys. Rev. A* **72**, 032309 (2005).
- [18] M. R. Dowling, A. C. Doherty, and S. D. Bartlett, Energy as an entanglement witness for quantum many-body systems, *Phys. Rev. A* **70**, 062113 (2004).
- [19] X. Wang, Threshold temperature for pairwise and many-particle thermal entanglement in the isotropic heisenberg model, *Phys. Rev. A* **66**, 044305 (2002).
- [20] T. Vértesi and E. Bene, Thermal entanglement in the nanotubular system $\text{Na}_2\text{V}_3\text{O}_7$, *Phys. Rev. B* **73**, 134404 (2006).
- [21] I. Siloi and F. Troiani, Towards the chemical tuning of entanglement in molecular nanomagnets, *Phys. Rev. B* **86**, 224404 (2012).
- [22] I. Siloi and F. Troiani, Quantum entanglement in heterometallic wheels, *The European Physical Journal B* **86**, 71 (2013).
- [23] F. Troiani and I. Siloi, Energy as a witness of multipartite entanglement in chains of arbitrary spins, *Phys. Rev. A* **86**, 032330 (2012).
- [24] T. Homayoun and K. Aghayar, Energy as an entanglement witnesses for one dimensional XYZ Heisenberg lattice: Optimization approach, *J. Stat. Phys.* **176**, 85 (2019).
- [25] F. Troiani, S. Carretta, and P. Santini, Detection of entanglement between collective spins, *Phys. Rev. B* **88**, 195421 (2013).
- [26] E. Barouch, B. M. McCoy, and M. Dresden, Statistical mechanics of the XY model. I, *Phys. Rev. A* **2**, 1075 (1970).
- [27] E. Barouch and B. M. McCoy, Statistical mechanics of the XY model. III, *Phys. Rev. A* **3**, 2137 (1971).
- [28] F. Iglói and H. Rieger, Long-range correlations in the nonequilibrium quantum relaxation of a spin chain, *Phys. Rev. Lett.* **85**, 3233 (2000).
- [29] K. Sengupta, S. Powell, and S. Sachdev, Quench dynamics across quantum critical points, *Phys. Rev. A* **69**, 053616 (2004).
- [30] A. Polkovnikov, K. Sengupta, A. Silva, and M. Vengalattore, Colloquium: Nonequilibrium dynamics of closed interacting quantum systems, *Rev. Mod. Phys.* **83**, 863 (2011).
- [31] S. Sotiriadis, D. Fioretto, and G. Mussardo, Zamolodchikov–faddeev algebra and quantum quenches in integrable field theories, *Journal of Statistical Mechanics: Theory and Experiment* **2012**, P02017 (2012).
- [32] G. Roux, Quenches in quantum many-body systems: One-dimensional bose-hubbard model reexamined, *Phys. Rev. A* **79**, 021608 (2009).
- [33] S. Sotiriadis, P. Calabrese, and J. Cardy, Quantum quench from a thermal initial state, *EPL (Europhysics Letters)* **87**, 20002 (2009).
- [34] M. Kollar and M. Eckstein, Relaxation of a one-dimensional mott insulator after an interaction quench, *Phys. Rev. A* **78**, 013626 (2008).
- [35] T. Barthel and U. Schollwöck, Dephasing and the steady state in quantum many-particle systems, *Phys. Rev. Lett.* **100**, 100601 (2008).
- [36] M. Cramer, A. Flesch, I. P. McCulloch, U. Schollwöck, and J. Eisert, Exploring local quantum many-body relaxation by atoms in optical superlattices, *Phys. Rev. Lett.* **101**, 063001 (2008).
- [37] M. Cramer, C. M. Dawson, J. Eisert, and T. J. Osborne, Exact relaxation in a class of nonequilibrium quantum lattice systems, *Phys. Rev. Lett.* **100**, 030602 (2008).
- [38] S. R. Manmana, S. Wessel, R. M. Noack, and A. Muramatsu, Strongly correlated fermions after a quantum quench, *Phys. Rev. Lett.* **98**, 210405 (2007).
- [39] M. A. Cazalilla, Effect of suddenly turning on interactions in the luttinger model, *Phys. Rev. Lett.* **97**, 156403 (2006).
- [40] P. Calabrese and J. Cardy, Time dependence of correlation functions following a quantum quench, *Phys. Rev. Lett.* **96**, 136801 (2006).
- [41] M. Rigol, V. Dunjko, V. Yurovsky, and M. Olshanii, Relaxation in a completely integrable many-body quantum system: An ab initio study of the dynamics of the highly excited states of 1d lattice hard-core bosons, *Phys. Rev. Lett.* **98**, 050405 (2007).
- [42] R. Hamazaki, T. N. Ikeda, and M. Ueda, Generalized gibbs ensemble in a nonintegrable system with an extensive number of local symmetries, *Phys. Rev. E* **93**, 032116 (2016).
- [43] J. Larson, Integrability versus quantum thermalization, *Journal of Physics B: Atomic, Molecular and Optical Physics* **46**, 224016 (2013).
- [44] V. A. Yurovsky and M. Olshanii, Memory of the initial conditions in an incompletely chaotic quantum system: Universal predictions with application to cold atoms, *Phys. Rev. Lett.* **106**, 025303 (2011).
- [45] M. Olshanii, K. Jacobs, M. Rigol, V. Dunjko, H. Kennard, and V. A. Yurovsky, An exactly solvable model for the integrability–chaos transition in rough quantum billiards, *Nature Communications* **3**, 641 (2012).
- [46] L. Vidmar and M. Rigol, Generalized gibbs ensemble in integrable lattice models, *Journal of Statistical Mechanics: Theory and Experiment* **2016**, 064007 (2016).
- [47] E. Ilievski, M. Medenjak, T. Prosen, and L. Zadnik, Quasilocal charges in integrable lattice systems, *Journal of Statistical Mechanics: Theory and Experiment* **2016**, 064008 (2016).
- [48] E. Ilievski, J. De Nardis, B. Wouters, J.-S. Caux, F. H. L. Essler, and T. Prosen, Complete generalized gibbs ensembles in an interacting theory, *Phys. Rev. Lett.* **115**, 157201 (2015).

- [49] F. H. L. Essler, G. Mussardo, and M. Panfil, Generalized gibbs ensembles for quantum field theories, *Phys. Rev. A* **91**, 051602 (2015).
- [50] B. Pozsgay, Failure of the generalized eigenstate thermalization hypothesis in integrable models with multiple particle species, *Journal of Statistical Mechanics: Theory and Experiment* **2014**, P09026 (2014).
- [51] G. Goldstein and N. Andrei, Failure of the local generalized gibbs ensemble for integrable models with bound states, *Phys. Rev. A* **90**, 043625 (2014).
- [52] B. Pozsgay, M. Mestyán, M. A. Werner, M. Kormos, G. Zaránd, and G. Takács, Correlations after quantum quenches in the xzx spin chain: Failure of the generalized gibbs ensemble, *Phys. Rev. Lett.* **113**, 117203 (2014).
- [53] B. Wouters, J. De Nardis, M. Brockmann, D. Fioretto, M. Rigol, and J.-S. Caux, Quenching the anisotropic heisenberg chain: Exact solution and generalized gibbs ensemble predictions, *Phys. Rev. Lett.* **113**, 117202 (2014).
- [54] P. Calabrese, F. H. L. Essler, and M. Fagotti, Quantum quench in the transverse field ising chain: I. time evolution of order parameter correlators, *Journal of Statistical Mechanics: Theory and Experiment* **2012**, P07016 (2012).
- [55] B. Blass, H. Rieger, and F. Iglói, Quantum relaxation and finite-size effects in the XY chain in a transverse field after global quenches, *EPL (Europhysics Letters)* **99**, 30004 (2012).
- [56] E. Lieb, T. Schultz, and D. Mattis, Two soluble models of an antiferromagnetic chain, *Ann. Phys.* **16**, 407 (1961).
- [57] P. Pfeuty, The one-dimensional ising model with a transverse field, *Ann. Phys.* **57**, 79 (1970).
- [58] M. Lewenstein, B. Kraus, P. Horodecki, and J. I. Cirac, Characterization of separable states and entanglement witnesses, *Phys. Rev. A* **63**, 044304 (2001).
- [59] B. M. Terhal, Detecting quantum entanglement, *Theoretical Computer Science* **287**, 313 (2002).
- [60] G. Vidal and R. F. Werner, Computable measure of entanglement, *Phys. Rev. A* **65**, 032314 (2002).
- [61] A. Sanpera, R. Tarrach, and G. Vidal, Local description of quantum inseparability, *Phys. Rev. A* **58**, 826 (1998).
- [62] S. Rana, Negative eigenvalues of partial transposition of arbitrary bipartite states, *Phys. Rev. A* **87**, 054301 (2013).
- [63] M. Greiner, O. Mandel, T. W. Hänsch, and I. Bloch, Collapse and revival of the matter wave field of a bose-einstein condensate, *Nature* **419**, 51 (2002).
- [64] B. Paredes, A. Widera, V. Murg, O. Mandel, S. Fölling, I. Cirac, G. V. Shlyapnikov, T. W. Hänsch, and I. Bloch, Tonks–girardeau gas of ultracold atoms in an optical lattice, *Nature* **429**, 277 (2004).
- [65] L. E. Sadler, J. M. Higbie, S. R. Leslie, M. Vengalattore, and D. M. Stamper-Kurn, Spontaneous symmetry breaking in a quenched ferromagnetic spinor bose–einstein condensate, *Nature* **443**, 312 (2006).
- [66] A. Lamacraft, Quantum quenches in a spinor condensate, *Phys. Rev. Lett.* **98**, 160404 (2007).
- [67] T. Kinoshita, T. Wenger, and D. S. Weiss, A quantum newton’s cradle, *Nature* **440**, 900 (2006).
- [68] S. Hofferberth, I. Lesanovsky, B. Fischer, T. Schumm, and J. Schmiedmayer, Non-equilibrium coherence dynamics in one-dimensional bose gases, *Nature* **449**, 324 (2007).
- [69] I. Bloch, J. Dalibard, and W. Zwerger, Many-body physics with ultracold gases, *Rev. Mod. Phys.* **80**, 885 (2008).
- [70] S. Trotzky, Y.-A. Chen, A. Flesch, I. P. McCulloch, U. Schollwöck, J. Eisert, and I. Bloch, Probing the relaxation towards equilibrium in an isolated strongly correlated one-dimensional bose gas, *Nature Physics* **8**, 325 (2012).
- [71] M. Cheneau, P. Barmettler, D. Poletti, M. Endres, P. Schauß, T. Fukuhara, C. Gross, I. Bloch, C. Kollath, and S. Kuhr, Light-cone-like spreading of correlations in a quantum many-body system, *Nature* **481**, 484 (2012).
- [72] T. W. Burkhardt and I. Guim, Finite-size scaling of the quantum ising chain with periodic, free, and antiperiodic boundary conditions, *Journal of Physics A: Mathematical and General* **18**, L33 (1985).
- [73] G. G. Cabrera and R. Jullien, Role of boundary conditions in the finite-size ising model, *Phys. Rev. B* **35**, 7062 (1987).